Theory of the NO+CO surface-reaction model

Adriana G. Dickman,* Bartira C. S. Grandi,† Wagner Figueiredo,‡ and Ronald Dickman§
Departamento de Física, Universidade Federal de Santa Catarina, Campus Universitário–Trindade, CEP 88040-900, Florianópolis-SC, Brazil
(Received 25 November 1998)

We derive a pair approximation (PA) for the NO+CO model with instantaneous reactions. For both the triangular and square lattices, the PA, derived here using a simpler approach, yields a phase diagram with an active state for CO-fractions y in the interval $y_1<y<y_2$, with a continuous (discontinuous) phase transition to a poisoned state at y_1 (y_2). This is in qualitative agreement with simulation for the triangular lattice, where our theory gives a rather accurate prediction for y_2. To obtain the correct phase diagram for the square lattice, i.e., *no* active stationary state, we reformulate the PA using *sublattices*. The (formerly) active regime is then replaced by a poisoned state with broken symmetry (unequal sublattice coverages), as observed recently by Kortlüke *et al.* [Chem. Phys. Lett. **275**, 85 (1997)]. In contrast with their approach, in which the active state persists, although reduced in extent, we report here the qualitatively correct theory of the NO+CO model on the square lattice. Surface diffusion of nitrogen can lead to an active state in this case. In one dimension, the PA predicts that diffusion is required for the existence of an active state. [S1063-651X(99)02406-X]

PACS number(s): 05.70.Ln, 82.65.Jv, 82.20.Mj, 05.70.Fh

I. INTRODUCTION

Following the introduction by Ziff, Gulari, and Barshad (ZGB) of a simple lattice model for the kinetics of the reaction $CO+1/2\ O_2\rightarrow CO_2$ on a catalytic surface, the study of surface reaction models has attracted increasing attention in nonequilibrium statistical physics [1]. Motivated by possible applications as well as intrinsic interest, the phase diagrams of a wide variety of models have been investigated in simulations and approximate, mean-fieldlike analyses. A typical feature is the existence of one or more absorbing states, i.e., configurations from which the system cannot escape [2]. Continuous phase transitions to an absorbing state fall generically in the class of directed percolation [3–5]. While this aspect is highly universal, other details of the phase diagram depend on very specific model-dependent properties such as steric or geometric effects, the possibility of nonreactive desorption, diffusion of, and interactions among, adsorbed species. Applied to surface reaction models, mean-field theories, particularly at the two-site or *pair* level, often provide reasonable qualitative predictions for the phase diagram.

In the present paper we derive pair mean-field approximations for one of the more complicated surface reaction models, that of NO+CO [6]. We briefly review its main features, deferring a precise definition to Sec. II. The catalytic surface (i.e., one of the platinum-group metals), is modeled by a regular lattice (typically square or triangular) of equivalent adsorption sites. This surface is exposed to a reservoir of CO and NO at fixed concentrations. While CO needs but a single vacant site, NO requires a nearest-neighbor pair of sites to adsorb. [We note that a more realistic model, for example of the NO+CO reaction on Pt(100), would permit NO to adsorb at a single site; a vacant neighbor is required for dissociation [7]. For a realistic description based on differential equations for the coverages, see Ref. [8].] The fundamental control parameter of the model is y, the probability that the next molecule arriving at the surface will be CO. One may also introduce nearest-neighbor hopping rates for the various adsorbed species. Nearest-neighbor CO-O and N-N pairs are highly reactive: if any form (by adsorption or diffusion), they are eliminated before anything else happens, and the products (CO_2 and N_2, respectively) desorb immediately.

On the triangular lattice (i.e., coordination number six), the phase diagram of the NO+CO model resembles that of the ZGB model: there is a reactive window for $y_1<y<y_2$, with a continuous phase transition at $y_1\approx 0.17$, and a discontinuous transition at $y_2\approx 0.35$ [6,9–11]. For y values outside the reactive window, the system eventually falls into an absorbing or ''poisoned'' configuration, devoid of vacant sites (the number of such configurations grows exponentially with system size). For $y<y_1$ the final configuration consists predominantly of O, with an appreciable fraction of N. [A special case is $y=0$, corresponding to a kind of random sequential adsorption (RSA) [12] of dimers, with partial reaction. The final state consists of O and N atoms, with isolated vacancies interspersed.] For $y>y_2$, CO takes over the role played by O in the small-y case. Diffusion of N, CO, and/or O shifts the transition points to some extent, but does not modify the phase diagram in any fundamental way.

On the square lattice, the picture is radically different, there being (without diffusion of N), *no* active stationary state, whatever the value of y [6,13–15]. This observation, based on Monte Carlo simulations, was explained by Brosilow and Ziff (BZ), who argued that the active state is

*Electronic address: dri@fisica.ufmg.br
†Electronic address: bartirag@fisica.ufsc.br
‡Electronic address: wagner@fisica.ufsc.br
§On leave of absence from Department of Physics and Astronomy, Herbert H. Lehman College, City University of New York, Bronx, NY 10468-1589. Electronic address: dickman@fisica.ufmg.br

unstable to the filling of one sublattice with N atoms [9]. Once this occurs, further adsorption of dimers is blocked, and the remaining vacancies are filled in with CO, yielding a poisoned configuration. While BZ cast their argument in terms of global sublattice filling, in practice the system poisons through the growth of local ''antiferromagnetic'' domains, i.e., patches having one or another sublattice filled with N. Since the dynamics stops once the domains fill the system, relaxation to a globally ordered state is not possible. For the same reason, no sharp transitions in coverages are observed as y is varied [6,13,14,9,10,16]. (It may be overstating the case to say that currently available results rule out any phase transition in the square lattice. Simulations show the coverages changing rapidly over a narrow range of y, but without discontinuities in the coverages or their slopes.) That the N-sublattice instability is responsible for destroying the active state (despite the absence of global sublattice order) is indicated by the observations that (i) an active state exists in the triangular lattice (which does not admit a decomposition into two sublattices), and (ii) that diffusion of N (but not of O, or of CO) restores the possibility of an active state [16,17].

Several theories of the NO+CO model have been proposed. Truncated at the 1-site level, the hierarchy of equations governing the cluster probabilities yields a reasonable estimate for y_2 on the triangular lattice [9,10], but places the continuous transition at $y_1=0$. Cortés *et al.* derived a pair approximation for the NO+CO model including CO desorption, using finite reaction rates [18]. Kortlüke, Kuzovkov, and von Niessen (KKN) derived a very accurate prediction for y_1 on the triangular lattice using a two-site cluster approximation [19].

None of the theories mentioned so far gives the phase diagram correctly for the square lattice: all predict an active state over some range of y. KKN made the fundamental observation that in this case, one must allow different concentrations on the two sublattices to have any hope of capturing the instability identified by BZ [19]. They devised a two-site cluster approximation incorporating sublattices, and obtained an active state of reduced extent, and a *third* transition point inside the (mainly) CO-poisoned phase. In other words, the theory of KKN, while representing an improvement on theories ignoring sublattices, remains at variance with simulation (and the BZ argument), in allowing an active state, and predicts a third, unobserved transition.

In this paper we formulate a pair approximation (PA) for the NO+CO model on the square and triangular lattices, as well as in one dimension; we retain the instantaneous reactions generally used in simulations. (While a theory employing a finite reaction rate k is simpler algebraically, its $k\to\infty$ limit is not equivalent to a theory with instantaneous reactions [20].) The standard PA predicts an active state for $0<y_1<y<y_2$; this is qualitatively correct for the triangular lattice, wrong for the square lattice. We obtain the correct phase diagram in the latter case from a pair approximation incorporating sublattices (PAS); the regime exhibiting activity in the PA now poisons via the sublattice instability. Our results for the coverages are in good accord with simulation, but due to the assumed homogeneity *within* each sublattice, phase transitions between different kinds of absorbing states persist at y_1 and y_2, and the order parameter (the difference in sublattice coverages), takes a nonzero value for $y_1<y<y_2$. We find that diffusion of N atoms lifts the instability, permitting an active state. But in our theory, the entire range $y_1<y<y_2$ becomes active once the diffusion rate D_N exceeds a critical value. In simulations the ''active window'' opens gradually as D_N is increased [16,17].

We have devised a simplified approach to deriving cluster mean-field equations. The method, which we illustrate with a simple example, proves particularly useful in the case of the NO+CO model, which allows 8 kinds of nearest-neighbor pairs, and up to 22 transitions among them. The remainder of this paper is organized as follows. Section II contains a definition of the model, including the reaction and diffusion steps. The PA method is described in Sec. III, with examples of its application to the contact process and the NO+CO reaction given in Appendices A and B, respectively. Our results are presented in Sec. IV, and a brief discussion follows in Sec. V.

II. MODEL

The NO+CO surface reaction model follows the Langmuir-Hinshelwood mechanism, in which both reacting species must be adsorbed on the substrate [21]. The steps below characterize the model [6]: (a) $CO(g)+V\to CO_a$, (b) $NO(g)+2V\to O_a+N_a$, (c) $2N_a\to N_2(g)+2V$, (d) $CO_a+O_a\to CO_2(g)+2V$, where A_a indicates an adsorbed species, A(g) a molecule in the gas phase, and V a vacant site. Steps (a) and (b) represent adsorption of carbon monoxide, and of nitric oxide, respectively. In step (c), two nearest-neighbor nitrogen atoms combine to form N_2(g), and in step (d), an oxygen atom reacts with a carbon monoxide molecule to form CO_2. N_2(g) and CO_2(g) desorb from the surface immediately. In this paper we assume complete dissociation of NO. (Various aspects of incomplete dissociation are considered in Refs. [16–18].) As noted above, reactions are assumed to occur instantaneously: nearest-neighbor CO-O and N-N pairs cannot reside on the lattice.

We now define the Markov process associated with the above set of reactions. On a lattice $\mathcal{L}$ comprising N sites, the state space of the process is the set of configurations $\{\sigma\}\equiv\{\sigma_i\}_{i\in\mathcal{L}}$, where the site variable σ_i takes values V, N, C, or O in case site i is vacant, or occupied by N, CO, or O, respectively. One trial (or sample path) of the process consists of a sequence of configurations $\{\sigma\}_0,\ldots,\{\sigma\}_{\mathcal{N}}$. A transition between configurations $\{\sigma\}_n$ and $\{\sigma\}_{n+1}$ is generated via the following steps: (i) Choose the identity of the next arriving molecule: CO with probability y, NO with probability $1-y$. (ii) In case of CO, choose a site $\mathbf{x}$; in case of NO, choose a nearest-neighbor pair $(\mathbf{x},\ \mathbf{y})$. If $\mathbf{x}$ (and/or $\mathbf{y}$, in the case of NO) is occupied in $\{\sigma\}_n$, then $\{\sigma\}_{n+1}=\{\sigma\}_n$, i.e., the configuration does not change. Otherwise, let $\{\sigma'\}$ be the configuration obtained by placing CO at $\mathbf{x}$, or in the NO case, N at $\mathbf{x}$ and O at $\mathbf{y}$. (iii) If $\{\sigma'\}$ contains no N-N or CO-O nearest-neighbor pairs, then $\{\sigma\}_{n+1}=\{\sigma'\}$. If $\{\sigma'\}$ does contain such pairs, they will react. Specifically, if the newly-arrived CO has m neighbors in state O, then one of these (chosen at random if $m>1$), as well as the CO, is removed from $\{\sigma'\}$ to give $\{\sigma\}_{n+1}$. In the

case of NO deposition, the analogous procedure is applied to the newly arrived N atom (if it has one or more neighbors N), and to the O atom (should it have any CO neighbors), to generate $\{\sigma\}_{n+1}$.

We associate with configuration $\{\sigma\}_n$ a ''time'' $t=n/N$. (This adds nothing to the process; it is convenient, nonetheless, to define a time unit comprising one attempted transition, on average, per lattice site. In simulations, it is often more efficient to choose the *first* site **x** for the adsorption step from a list of currently vacant sites. But in this case, the time increment associated with the transition from $\{\sigma\}_n$ to $\{\sigma\}_{n+1}$ is $\Delta t=1/\mathcal{V}_n$ where $\mathcal{V}_n$ is the number of vacant sites in $\{\sigma\}_n$.)

To our knowledge, all of the simulations of the NO+CO model cited herein treat the Markov process defined above. (The constant-coverage studies of BZ clearly follow a different procedure, but the stationary properties of the two processes should converge in the large-size limit [9].) In the case of diffusion, however, various definitions have been employed. Here, we implement diffusion of (for example, N atoms) by modifying steps (i)–(iii) as follows. Prior to (i), we impose (a) Choose the process: diffusion with probability $D/(1+D)$, adsorption with probability $1/(1+D)$. In the latter case, proceed to steps (i)–(iii) as above. In the former, perform instead: (b) Choose a site **x** at random. If **x** is *not* occupied by N, then $\{\sigma\}_{n+1}=\{\sigma\}_n$. Otherwise, choose a neighbor **y** of **x** at random. If **y** is occupied, $\{\sigma\}_{n+1}=\{\sigma\}_n$. Otherwise, let $\{\sigma'\}$ be $\{\sigma\}_n$ with **x** vacant and **y** occupied by N. (c) If $\{\sigma'\}$ is free of N-N pairs, $\{\sigma\}_{n+1}=\{\sigma'\}$. Otherwise, choose a reacting pair, as in step (iii) above, to generate $\{\sigma\}_{n+1}$. This procedure is not calculated to optimize computational efficiency, but rather to provide a meaning for the parameter D that is *independent of the configuration*. The rate of hopping attempts of an adsorbed N atom is $D/(1+D)$. Diffusion processes for other species are defined analogously.

III. PAIR APPROXIMATION

Before considering the NO+CO model in detail, we explain a simplified method for deriving the PA equations. These equations govern the evolution of the probabilities $P(ij,t)$, that a randomly chosen nearest-neighbor pair of sites, **x** and **x**′, say, are in states i and j. In most previous treatments, (see, for example Ref. [22]), the rates of change of the $P(ij)$ are derived by enumerating the changes in the number of nearest-neighbor pairs in a *neighborhood* of sites centered on, and including, a central pair. For example, in a one-dimensional system with nearest-neighbor interactions and two states, ''0'' and ''1,'' per site, a transition of the form $(0011)\rightarrow(0111)$ occurs at rate $P(0011)w(001\rightarrow011)$. Counting the changes in the central pair *and* the periphery, we see that in this process, one (11) pair is created and one (00) pair destroyed. The simplification comes from *ignoring* changes outside the central pair, and regarding the above process as one in which $(01)\rightarrow(11)$. Since $P(ij)$ is the probability for *any* nearest-neighbor pair, following the changes at a particular pair (e.g., the central one), is sufficient. This results in a significant reduction in bookkeeping, particularly in two or more dimensions, and for processes (such as the NO+CO model) in which a fairly large number of peripheral sites can influence the transition probabilities. We illustrate the method by applying it to the contact process in Appendix A.

In the table below we list the allowed (x) and forbidden (⊘) nearest-neighbor pairs in the NO+CO model. (Entries below the main diagonal are redundant.)

	V	*N*	*C*	*O*
V	x	x	x	x
N		⊘	x	x
C			x	⊘
O				x

Next we require the set of transitions between pairs. In the table below, we assign arbitrary labels to the allowed transitions, and leave the remaining fields blank. For the square lattice only processes 1–20 are pertinent, 21 and 22 being possible only on the triangular lattice. In one dimension, transition 4 is also excluded. Diffusion alters the rates, but not the set of possible transitions, the only exception being when we consider sublattices.

To \ From	*VV*	*VN*	*VC*	*VO*	*NC*	*NO*	*CC*	*OO*
VV		1	2	3	4			
VN	5		21		6	7		
VC	8				9		10	
VO	11	22				12		13
NC		14	15					
NO	16	17		18				
CC			19					
OO				20				

The heart of the calculation lies in deriving expressions for the transition rates $R_1, \ldots, R_{22}$. Once these are in hand, we can write the equations for the pair probabilities by noting that each transition acts as a source for one pair (i.e., in the first column of the table), and a loss term for another (listed in the top row). Denoting the pair probabilities by (ij), where i and j can be V, N, C, or O, we have, for example, that

$$\frac{d(VN)}{dt} = R_5 + R_6 + R_7 + R_{21} - R_1 - R_{14} - R_{17} - R_{22}, \quad (1)$$

and

$$\frac{d(VV)}{dt} = 2[R_1 + R_2 + R_3 + R_4 - R_5 - R_8 - R_{11} - R_{16}], \quad (2)$$

the overall factor of two arising, in the last expression, due to contributions in which the molecules (always of different species, in this case) occur in the opposite order. Here it is important to emphasize that for $i \neq j$, (ij) represents the probability to find a site $\mathbf{x}$ in state i, and its neighbor $\mathbf{y}$ in state j; (ji), which represents the reversed situation, is of course equal to (ij) by symmetry. Thus the normalization condition reads

$$(VV) + (CC) + (OO) + 2[(VN) + (VC) + (VO) + (NC) + (NO)] = 1. \quad (3)$$

We introduce a similar notation for site probabilities:

$$(V) = (VV) + (VN) + (VC) + (VO), \quad (4)$$

$$(N) = (NV) + (NC) + (NO), \quad (5)$$

$$(C) = (CV) + (CN) + (CC), \quad (6)$$

and

$$(O) = (OV) + (ON) + (OO). \quad (7)$$

Another useful piece of notation represents the probability of having site $\mathbf{x}$ in state i and its neighbor *not* in state j by $(i\not{j})$. For example,

$$(V\not{N}) = (VV) + (VO) + (VC), \quad (8)$$

and

$$(C\not{C}) = (CV) + (CN). \quad (9)$$

Finally, when employing sublattices A and B, we use $(i)_A$ to denote the site probability of i in sublattice A [similarly for $(i)_B$], and $(ij)_A$ to denote the probability of finding a site in state i in the A sublattice, and its neighbor (in B), in state j. $(i\not{j})_A$ is defined analogously. In a sublattice calculation we have thirteen different pair probabilities, since for $i \neq j$ we must distinguish $(ij)_A$ and $(ij)_B$. [By definition, $(ij)_A = (ji)_B$.] Diffusion introduces one further transition beyond those enumerated above: if species i can perform nearest-neighbor hopping, the transition $(iV)_A \rightarrow (iV)_B$ becomes possible.

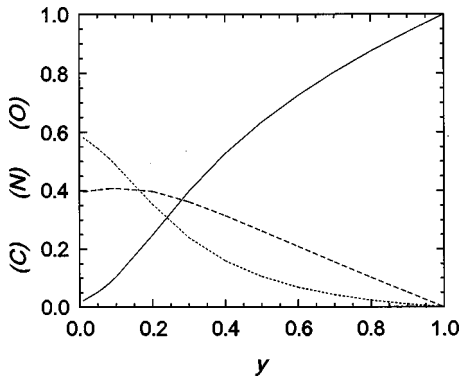

FIG. 1. Coverages versus y in one dimension in the absence of diffusion. Solid line, (C); dotted line, (O); dashed line, (N).

Each (nondiffusive) event involves the arrival of a molecule, either CO or NO, at the surface. Since the next arriving molecule is CO with probability y, rates for processes involving the arrival of CO carry a factor of y. In processes involving the arrival of NO, we require the probability that the next event involves N arriving at a certain site $\mathbf{x}$, and, of course, O arriving at a neighbor $\mathbf{y}$. In a lattice with coordination number z, this probability is $\tilde{y} \equiv (1-y)/z$.

The expressions for the various rates are, in general, quite complicated, and we shall not list all of them here. Examples of their derivation are given in Appendix B [23]. The PA equations are integrated numerically, using a fourth-order Runge-Kutta scheme [24], starting from an empty lattice.

IV. RESULTS

A. One dimension

Applied to the NO+CO model on a line, the PA predicts no active steady state in the absence of diffusion (see Fig. 1). The dependence of the coverages on y is qualitatively similar to that found in simulations of the square lattice [10,16]. The vacancy fraction is nonzero only for $y=0$, where we find $(V)=0.1623$, $(O)=0.5013$, and $(N)=0.3364$ in the stationary state. In fact, the final vacancy concentration should be the same as in one-dimensional dimer RSA (without reaction), i.e., $(V)=e^{-2}=0.13534\ldots$ [25]. This is because a N-N reaction always yields the configuration $OVVO$. The vacancy pair is subsequently filled in, so the sum of the final coverages, $(N)+(O)$, is identical to the final O coverage in RSA of O_2 [26]. While the PA is exact for dimer RSA in one-dimension (due to a shielding property [12]), in the present case the approximation cannot deal adequately with the reactions. The configuration VNV, for example, is impossible in the pure-NO process (each N has at least one O neighbor), but is assigned a nonzero probability in the PA. We obtain better results for the final coverages from a three-site approximation: $(V)=0.1486$, $(O)=0.5001$, and $(N)=0.3505$. (The KKN method yields a further slight improvement: $(V)=0.1453$, $(O)=0.5095$, $(N)=0.3452$; simulations yield $(V)=0.1353$, $(O)=0.5066$, and $(N)=0.3581$ [27].)

Next we consider the effect of a nonzero diffusion rate, D_N, of N_a atoms. For $D_N > D_N^c = 4.38$, we find a reactive window for $y_1 < y < y_2$, with a continuous (discontinuous)

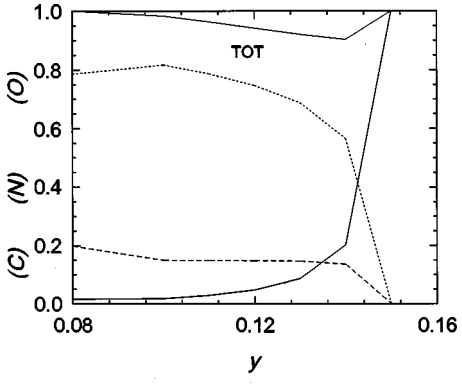

FIG. 2. Coverages versus y in one dimension, for $D_N=10.0$. Symbols as in Fig. 1.

transition at y_1 (y_2). Figure 2 shows the coverages for $D_N=10.0$. In Fig. 3 we plot $\Delta \equiv y_2 - y_1$ as a function of D_N. With increasing D_N, y_1 tends to zero and y_2 to 0.2. Close to D_N^c, Δ is described, approximately, by $\Delta \sim (D_N - D_N^c)^{0.67}$. For diffusion of CO (but none of the other species), we find an active state for $D_{CO} \geqslant D_{CO}^c = 7.19$. The width, which is very small, grows linearly with D_{CO} in the neighborhood of the critical value. Both y_1 and y_2 shift to higher values with increasing D_{CO}. Finally, for diffusion of O atoms (exclusively), we find $D_O^c = 0.75$. The window width follows $\Delta \approx (D_O - D_O^c)^{0.24}$ in the vicinity of D_O^c. The continuous transition ($y = y_1$) always occurs near $y = 0$; for large values of D_O, y_2 approaches a limiting value of 0.27. We note that for $y = 0$, even very small values of D_O cause a drastic reduction in the fraction of vacant sites: when $D_O = 0.05$, for example, $(V) < 10^{-4}$; for $D_O = 16.0$, $(V) < 10^{-6}$. Similar behavior is observed in simulations on the triangular lattice [17].

B. Triangular lattice

The coverages predicted by our method for the NO+CO model (without diffusion) on the triangular lattice are compared against simulation results [10] in Fig. 4. There is an active steady state between the continuous transition at $y_1 = 0.040(1)$, and $y_2 = 0.363(1)$, which marks a discontinuous transition. (We note that the latter is the result for an initially empty lattice. Commencing with a finite CO coverage will, in general, yield a smaller value for y_2.) The table below compares our PA results for the transition points with those predicted by the site approximation (SA) [9,10], and the KKN method [19], and found in simulations [9].

	SA	KKN	PA	Simulation
y_1	0.0	0.152(1)	0.040	0.1725(25)
y_2	0.3877	0.393(1)	0.363	0.3514(1)

While our result for y_2 is in good agreement with simulation, we obtain a poor estimate for y_1. The latter is a consequence of neglecting explicit correlations beyond nearest neighbors in the pair approximation, and, perhaps, of ignoring certain nearest-neighbor pair factors in reckoning cluster probabilities (see Appendix B). For $y = 0$ we find a final poisoned state characterized by $(O) = 0.8538$, $(N) = 0.1462$, and $(V) \simeq 2 \times 10^{-6}$. Simulations yield $(O) = 0.7443$, $(N) = 0.1656$, and $(V) = 0.0901$ [28]. Clearly the PA does not give an accurate description of this RSA process with partial reaction, for either the triangular or square lattices (see below). (This is in contrast to pure dimer deposition, for which the PA does reasonably well [22].) Despite these discrepancies, the PA coverages are generally in good agreement with simulation.

C. Square lattice

The PA prediction for the phase diagram is qualitatively similar to that found for the triangular lattice. The continuous transition from a predominantly O-poisoned state to an active state occurs at $y_1 = 0.111$, and the discontinuous transition falls at $y_2 = 0.2981$. (The latter, again, is determined using an initially empty lattice.) Cortés *et al.* obtained $y_1 \approx 0.09$ and $y_2 \approx 0.35$ in this case, showing that the large-reaction-rate limit of a calculation using finite rates yields results comparable, but not identical to, one employing instantaneous reactions. (While the comparison is academic in the present instance, there being no active state on the square lattice, it is of interest to gauge the agreement between the two methods.) For $y = 0$ we obtain $(O) = 0.6551$ and $(N) = 0.0198$, while simulations yield $(O) = 0.6495$ and $(N) = 0.2416$ [28].

Since the PA predicts no active state in one dimension (in the absence of diffusion), it is interesting to check whether removing reaction 4, which is impossible in one dimension,

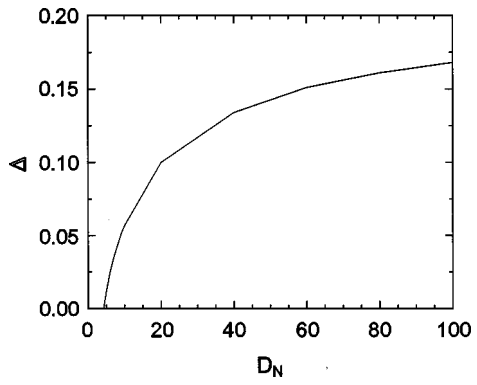

FIG. 3. Width of the reactive window in one dimension, as a function of the diffusion rate D_N. The critical value $D_N^c = 4.38$.

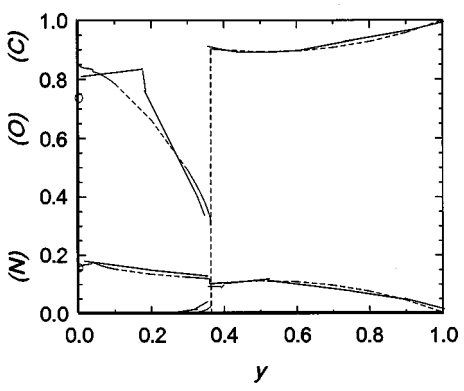

FIG. 4. Coverages in the triangular lattice. Solid lines, simulation (Ref. [10]); dashed lines: PA.

changes the phase diagram. We find that deleting this process has a minimal effect on the PA prediction for the square lattice. The cause for the dramatic difference between the linear and square lattice results must be sought elsewhere. (It is worth remarking that the PA similarly yields only absorbing states for the one-dimensional ZGB model.)

Introducing sublattices in the PA calculation (yielding what we call the PAS theory), changes the result drastically. We find that the active state predicted by the PA is *unstable* to the formation of N-rich and N-poor sublattices; in the process, the vacancy density falls to zero, and the active state vanishes. As detailed in Appendix B, we employ an extended set of variables, i.e., for $i \neq j$, $(i,j=V,N,C,$ or $O)$, probabilities $(ij)_A$ and $(ij)_B$, representing species i in the A or the B sublattice. [Naturally, the site coverages $(N)_A$ and $(N)_B$, etc., may also differ.] We begin the calculation, as before, with an empty lattice; the pair equations reach the same steady solutions as in the simple PA. For $y_1 < y < y_2$, we then probe the stability of the active state by transferring a small amount, $\Delta(N) \equiv (N)_A - (N)_B = 10^{-3}$, of N from one sublattice to the other, and study the response to this small perturbation. We find, in all cases, that $\Delta(N)$ grows, and that (V) decreases, finally becoming zero, that is, the PAS equations reach an absorbing state. Essentially identical results are obtained if we start from a slightly asymmetric initial condition, i.e., with a small N coverage on one of the sublattices, as was done in Ref. [19]. (We note in passing that introducing sublattices in the *site* approximation has no effect on the results.)

The PAS, then, represents the simplest theoretical approach giving a phase diagram in accord with simulation, for the NO+CO model on the square lattice. But it retains some of the undesirable features of the PA. Figure 5 shows that for $y < 0.1$, and again for $y > 0.5$, the PAS coverages are in good agreement with simulation. In these regimes, of course, the PA and PAS are identical (they only differ on the interval where the PA predicts an active state). For $0.1 < y < 0.5$ there are substantial differences between theory and simulation, associated with the continued appearance of phase transitions at y_1 and y_2 in the PAS. For $y_1 < y < y_2$ the PAS equations exhibit spontaneous symmetry breaking [19] associated with global ''antiferromagnetic'' order, $\Delta(N) \neq 0$ (see Fig. 6), which, as we have remarked, is not seen in simulations.

A final point concerns the effect of N diffusion on the phase diagram. Since this process tends to equalize the sublattice coverages, it is reasonable to expect an active state for sufficiently large values of D_N. This is indeed observed in simulations [16,29], where the range Δ of y values supporting an active state grows steadily with D_N. (The PA, as we have noted, yields a similar result in one dimension.) When we include N diffusion in the PAS calculation, we observe no active state for $D_N < D_N^c \simeq 0.023$, but for larger diffusion rates the entire interval between y_1 and y_2 becomes active at once.

V. DISCUSSION

We have formulated a pair approximation (PA) for the NO+CO surface reaction model with instantaneous reactions, using a simplified derivation. The PA gives quite reasonable predictions for coverages on the triangular lattice,

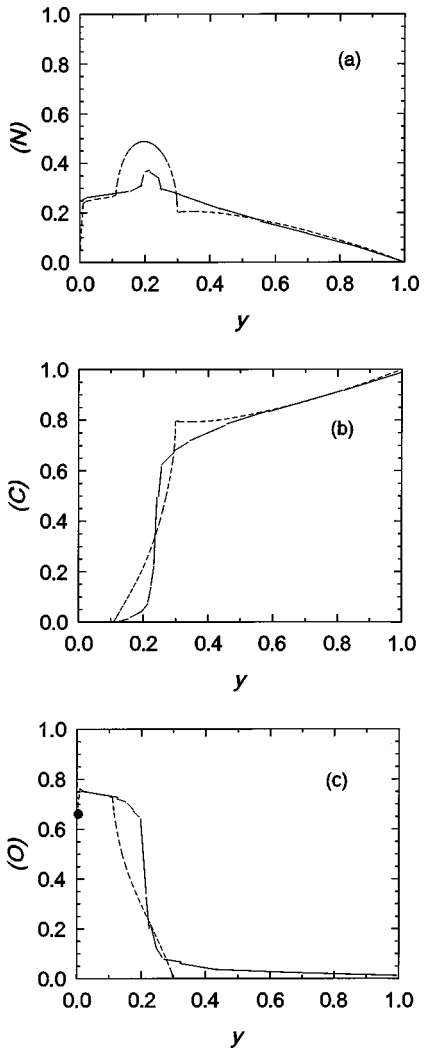

FIG. 5. (a) N coverage in the square lattice. Solid line, simulation (Ref. [10]); dashed line, PAS. (b) CO coverage, symbols as in (a); (c) O coverages, symbols as in (a).

but a surprisingly low value for the continuous transition point, y_1. The pair approximation with sublattices (PAS) gives a qualitatively correct phase diagram for the square lattice, but certain anomalous features of the simple PA persist, notably, singular behavior of the coverages at the transition points y_1 and y_2.

Our study shows that the PA can furnish reliable qualita-

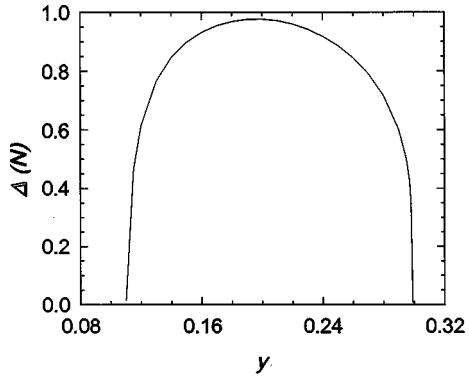

FIG. 6. PAS sublattice order parameter $\Delta(N)$.

tive, and in some instances quantitative predictions for reaction models, *provided it includes a mechanism for realizing any symmetry-breaking tendency inherent in the model*. The same condition applies, of course, to mean-field or cluster approximations for equilibrium models. In general, it is asking too much of such theories to provide quantitatively reliable phase boundaries; the PA may nonetheless yield some insight into the overall shape of the phase diagram. More accurate theories are typically based on the hierarchy of *n*-point functions.

The theory of KKN yields a remarkably accurate prediction for y_1 on the triangular lattice. This indicates that the effect of long-range correlations is reasonably well represented in their theory. Surprisingly, the PA yields a better prediction for y_2. It remains to develop a method that combines the advantages of the two approaches.

ACKNOWLEDGMENTS

We are grateful to Robert M. Ziff and Olaf Kortlüke for very helpful correspondence, and for providing us with simulation data prior to their publication. We thank Jim Evans for valuable correspondence. A.G.D. and W.F. are supported by CNPq (Brazil). We thank FINEP for financial support.

APPENDIX A: SIMPLIFIED DERIVATION OF PAIR EQUATIONS

Here we illustrate our method by applying it to the contact process (CP) [30]. The CP is a Markov process defined on a *d*-dimensional cubic lattice. Each site is either vacant (0) or occupied (1). The transition rates at any site are $w(1\to0)=1$ (independent of the neighbors) and $w(0\to1)=\lambda n/2d$, where $0\leqslant n\leqslant 2d$ is the number of neighboring sites in state 1. (Note that all sites 0 is an absorbing configuration.) Thus in one dimension we have $w(101\to111)=\lambda$, $w(100\to110)=w(001\to011)=\lambda/2$, and $w(000\to010)=0$. We enumerate below the transitions, associated rates (e.g., the transition rate times the probability of the initial configuration), and overall changes in the number of 1's and 11 nearest-neighbor pairs, in the one-dimensional CP. We use (1) to denote the density of 1's, (10) for the probability of a nearest-neighbor 0–1 pair, etc. (By normalization, $(00)+2(01)+(11)=1$. Note that the second and fourth entries carry a factor of 2 to account for mirror-image events.)

Process	Rate	ΔN_1	ΔN_{11}
$101\to111$	$\lambda(01)^2/(0)$	$+1$	$+2$
$100\to110$	$2\lambda(01)(00)/(0)$	$+1$	$+1$
$111\to101$	$(11)^2/(1)$	-1	-2
$110\to100$	$2\,(11)(01)/(1)$	-1	-1
$010\to000$	$(01)^2/(1)$	-1	0

Collecting results, one finds

$$\frac{d(1)}{dt}=\lambda[(1)-(11)]-(1), \tag{A1}$$

and

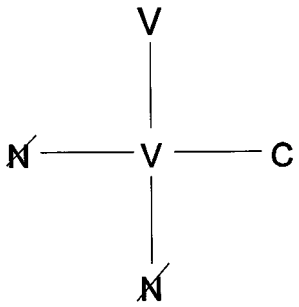

FIG. 7. One of three equivalent configurations required for the transition $VC\to NC$ in the square lattice.

$$\frac{d(11)}{dt}=\lambda\frac{(1)-(11)}{(0)}[1-(11)]-2(11). \tag{A2}$$

In this approximation, an active stationary solution [one with $(1)>0$], exists only for $\lambda>\lambda_c=2$. The above calculation is simple enough in one dimension, but becomes more complicated for higher *d*. We illustrate our simpler alternative method below on the *d*-dimensional CP. Only transitions at the central pair are enumerated. The rates involving creation receive independent contributions from within the pair (if it is of type 01) *and* from the $2d-1$ neighbors outside. (This independence is, of course, an approximation intrinsic to the PA.)

Transition	Rate
$11\to01$	$R_1=(11)$
$01\to11$	$R_2=\lambda(01)[1+(2d-1)(01)/(0)]/2d$
$10\to00$	$R_3=(10)$
$00\to10$	$R_4=(2d-1)\lambda(00)(01)/2d(0)$

We find $d(11)/dt=2[R_2-R_1]$, which reduces to Eq. (A2) for $d=1$, when we note that $(01)=(1)-(11)$. Noting that $(1)=(11)+(10)$, we immediately recover Eq. (A1) for any *d*. (Analysis of the stationary solutions shows that $\lambda_c=2d/(2d-1)$ in *d* dimensions.)

APPENDIX B: RATES FOR THE NO+CO MODEL

In this appendix we present several examples of the pair approximation (PA) transition rates for the NO+CO model, first on the square, and then on the triangular lattice. We begin with transition 15, $VC\to NC$, on the square lattice. Figure 7 shows one of three equivalent configurations needed to realize this process. The rate (per bond of the lattice) carries the factors (VC) (probability of the initial state) and $\tilde{y}$ (probability of NO arriving with N falling at the central vacant site). There are three possible locations (neighbors of V) at which O might adsorb; each is vacant, in the PA, with probability $(VV)/(V)$. (Whether the O atom reacts or not is unimportant in this instance.) If either of the remaining neighbors of V harbors an N atom, the newly arrived N will react. (Recall that we are considering *infinite* reaction rates in this paper.) Hence, these two sites must be free of N for the desired transition to occur, implying a factor of $[(V\not{N})/(V)]^2$. Thus,

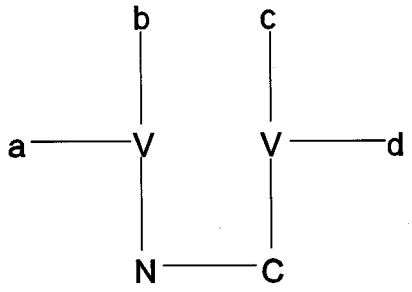

FIG. 8. One of two equivalent configurations required for the transition $NC \rightarrow VV$ in the square lattice.

$$R_{15} = 3\tilde{y}\frac{(VC)(VV)(V\mathbb{N})^2}{(V)^3}. \tag{B1}$$

Now suppose that N atoms can hop to neighboring sites at rate D_{N}. If one of the neighbors of V harbors an N atom, it can hop to the vacant site, and will remain there if the other neighbors are free of N. We must then add to the above expression the diffusive contribution

$$D_{15} = \frac{3D_{\mathrm{N}}}{4}\frac{(VC)(VN)(V\mathbb{N})^2}{(V)^3}, \tag{B2}$$

the factor of 1/4 reflecting the four possible directions of the attempted hopping move. (Note that we absorb a factor of $1+D_{\mathrm{N}}$ into a rescaled time variable.)

If we consider sublattices, each process splits in two. For process 15, the rate (including diffusion) for the case in which V lies in the A sublattice is readily seen to be

$$R_{15,A} = 3\tilde{y}\frac{(VC)_A(VV)(V\mathbb{N})_A^2}{(V)_A^3} + \frac{3D_N}{4}\frac{(VC)_A(VN)_A(V\mathbb{N})_A^2}{(V)_A^3}. \tag{B3}$$

(For any i, $R_{i,B}$ is found by interchanging A's and B's in $R_{i,A}$.)

A somewhat more complicated transition is number 4, $NC \rightarrow VV$. It is contingent upon an NO landing parallel to the central NC pair, with the two N's adjacent. One of two equivalent initial configurations is shown in Fig. 8. The solid lines indicate the pairs included in reckoning the probability of the configuration. Notice that when a pair of neighboring sites, **x** and **y**, are both neighbors of sites in the central pair, we use the pair factor associated with the central pair [$(VN)(VC)$ in this example], in preference to the factor between **x** and **y** [either $(VN)(VV)$ or $(VC)(VV)$]. We apply this rule in all our calculations, to eliminate possible ambiguities. Consider the neighbors **a** and **b** of the vacant site above N. If neither of these bear N, the newly arrived N will surely react with the N in the central pair. If either **a** or **b** (but not both) carry an N, the probability of the desired reaction is 1/2; it is 1/3 in case both **a** and **b** bear N. The probabilities of these events—no N, one N, or two—given the vacant neighbor, are $(V\mathbb{N})^2/(V)^2$, $2(V\mathbb{N})(VN)/(V)^2$, and $(VN)^2/(V)^2$, respectively. An analogous consideration applies to the probability of reaction of the central-pair CO, depending upon the presence of CO at **c** and/or **d**. Combining these observations, we arrive at

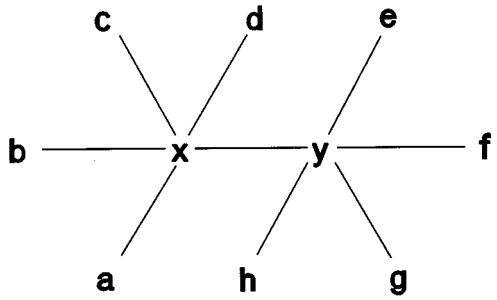

FIG. 9. Lines indicate the pair factors included in reckoning the probability of a set of ten sites in the triangle lattice.

$$R_4 = 2\tilde{y}\frac{(NC)(VN)(VC)}{(N)(C)(V)^4}\left[(V\mathbb{N})(V) + \frac{1}{3}(VN)^2\right] \times \left[(V\mathbb{C})(V) + \frac{1}{3}(VC)^2\right], \tag{B4}$$

where we used $(V\mathbb{N})+(VN)=(V)$ and $(V\mathbb{C})+(VC)=(V)$. For the sublattice calculation,

$$R_{4,A} = 2\tilde{y}\frac{(NC)_A(VN)_B(VC)_A}{(N)_A(C)_B(V)_A^2(V)_B^2}\left[(V\mathbb{N})_B(V)_B + \frac{1}{3}(VN)_B^2\right] \times \left[(V\mathbb{C})_A(V)_A + \frac{1}{3}(VC)_A^2\right]. \tag{B5}$$

There is no diffusive contribution to this process.

While several rates have more complicated expressions, all of the calculations in the square lattice follow the lines of those illustrated above. A new question of principle does arise in the triangular lattice, where it is not possible to include all the pair factors between the central pair of sites and their nearest neighbors in the simple PA. In the triangular lattice, if **x** and **y** are nearest neighbors, they have two neighbors (sites **d** and **h** in Fig. 9), *in common*. In the PA, the probability of finding **x**, **y**, and **d** in states i, j, and k, respectively, may be written as $(ij)(ik)/(i)$, $(ij)(jk)/(j)$, or $(ik)(kj)/(k)$, but *not* as $(ij)(ik)(jk)/(i)(j)(k)$. (The latter family of expressions is not, in general, even normalized!) Our choice of which pair factors to include is shown in Fig. 9. Note that as we sum over all the possible states of the peripheral sites, symmetry under the interchange of **x** and **y** is restored.

As an example, consider process 19, $VC \rightarrow CC$ (site **x** vacant and **y** occupied by CO in Fig. 9). A CO molecule must land at **x** and remain there, which implies that sites **a**, **b**, and **c** must be free of O. (Sites **d** and **h** have no possibility of bearing O, as they are neighbors of a site occupied by CO. The states of sites **e**, **f**, and **g** are unimportant in this

process.) Multiplying the independent factors associated with the events enumerated above, we find that the rate for this process is given by

$$R_{19}=y(VC)\frac{(V\emptyset)^3}{(V)^3}. \tag{B6}$$

A more complicated process is number 20, $VO \rightarrow OO$ (**x** vacant, **y** occupied by O in Fig. 9). An NO must fall with O at **x**, and N at one of the sites in $\{\mathbf{a},\mathbf{b},\mathbf{c},\mathbf{d},\mathbf{h}\}$. In no case may any of the sites in $\{\mathbf{a},\mathbf{b},\mathbf{c}\}$ hold CO. (Being neighbors of an O, **d** and **h** are surely free of CO.) The rate is given by the expression:

$$R_{20}=\tilde{y}(VO)\left\{3\frac{(VV)}{(V)}\left(\frac{(V\mathbb{C})}{(V)}\right)^2+\frac{(VV)}{(V\mathbb{C})}\left(\frac{(V\mathbb{C})}{(V)}\right)^3+\frac{(VO)}{(O)}\left(\frac{(V\mathbb{C})}{(V)}\right)^3\right\}. \tag{B7}$$

The first term in brackets represents N falling at **a**, **b**, or **c**. The next is for N falling at **d**. The probability of **d** being vacant, given one vacant neighbor and one occupied by O, is $(VV)/[(VV)+(VN)+(VO)]=(VV)/(V\mathbb{C})$. The final term represents N falling at **h**. These examples illustrate the principles used in the calculation, the resulting expressions, needless to say, become quite involved in certain cases.

[1] R. M. Ziff, E. Gulari, and Y. Barshad, Phys. Rev. Lett. **56**, 2553 (1986).

[2] R. Dickman, in *Nonequilibrium Statistical Mechanics in One Dimension*, edited by V. Privman (Cambridge University Press, Cambridge, 1996); J. Marro and R. Dickman, *Nonequilibrium Phase Transitions in Lattice Models* (Cambridge University Press, Cambridge, 1999).

[3] J. L. Cardy and R. L. Sugar, J. Phys. A **13**, L423 (1980); P. Grassberger, Z. Phys. B **47**, 365 (1982); H. K. Janssen, *ibid.* **42**, 151 (1981).

[4] P. Grassberger and A. De La Torre, Ann. Phys. (N.Y.) **122**, 373 (1979).

[5] G. Grinstein, Z.-W. Lai, and D. A. Browne, Phys. Rev. A **40**, 4820 (1989).

[6] K. Yaldram and M. A. Khan, J. Catal. **131**, 369 (1991).

[7] B. Meng, W. H. Weinberg, and J. W. Evans, J. Chem. Phys. **101**, 3234 (1994).

[8] T. Fink, J.-P. Dath, R. Imbihl, and G. Ertl, J. Chem. Phys. **95**, 2109 (1991).

[9] B. J. Brosilow and R. M. Ziff, J. Catal. **136**, 275 (1992).

[10] B. Meng, W. H. Weinberg, and J. W. Evans, Phys. Rev. E **48**, 3577 (1993).

[11] I. Jensen, J. Phys. A **27**, L61 (1994).

[12] J. W. Evans, Rev. Mod. Phys. **65**, 1281 (1993).

[13] K. Yaldram and M. A. Khan, J. Catal. **136**, 279 (1992).

[14] K. Yaldram and M. A. Khan, J. Phys. A **26**, 6135 (1993).

[15] K. Yaldram and M. A. Khan, J. Phys. A **26**, L801 (1993).

[16] M. A. Khan, K. Yaldram, G. K. Khalil, and K. M. Khan, Phys. Rev. E **50**, 2156 (1994).

[17] O. Kortlüke and W. von Niessen, J. Chem. Phys. **105**, 4764 (1996).

[18] J. Cortés, H. Puschmann, and E. Valencia, J. Chem. Phys. **109**, 6086 (1998).

[19] O. Kortlüke, V. N. Kuzovkov, and W. von Niessen, Chem. Phys. Lett. **275**, 85 (1997).

[20] J. W. Evans, Langmuir **7**, 2514 (1991).

[21] H. Oh, B. B. Fisher, J. E. Carpenter, and D. Goodman, J. Catal. **100**, 360 (1986).

[22] R. Dickman, Phys. Rev. A **34**, 4246 (1986).

[23] We shall be happy to supply detailed rate expressions and/or computer codes for integration of the PA equations to interested readers.

[24] W. H. Press, B. P. Flannery, S. A. Teukolsky, and W. T. Vetterling, *Numerical Recipes* (Cambridge University Press, Cambridge, 1996).

[25] P. J. Flory, J. Am. Ceram. Soc. **61**, 1518 (1939).

[26] We thank Olaf Kortlüke for pointing this out.

[27] O. Kortlüke (unpublished).

[28] R. M. Ziff (unpublished).

[29] O. Kortlüke and W. von Niessen, Surf. Sci. **401**, 185 (1998).

[30] T. E. Harris, Ann. Prob. **2**, 969 (1974).